

## Reversal of Simple Hydrogenic Isotope Scaling Laws in Tokamak Edge Turbulence

E. A. Belli<sup>1</sup>,\* J. Candy<sup>1</sup>, and R. E. Waltz<sup>1</sup>

General Atomics, P.O. Box 85608, San Diego, California 92186-5608, USA



(Received 23 March 2020; accepted 9 June 2020; published 30 June 2020)

The role of nonadiabatic electrons in regulating the hydrogenic isotope-mass scaling of gyrokinetic turbulence in tokamak fusion plasmas is assessed in the transition from ion-dominated core transport regimes to electron-dominated edge transport regimes. We propose a new isotope-mass scaling law that describes the electron-to-ion mass-ratio dependence of turbulent ion and electron energy fluxes. The mass-ratio dependence arises from the nonadiabatic response associated with fast electron parallel motion and plays a key role in altering—and in the case of the DIII-D edge, favorably reversing—the naive gyro-Bohm scaling behavior. In the reversed regime hydrogen energy fluxes are larger than deuterium fluxes, which is the opposite of the naive prediction.

DOI: 10.1103/PhysRevLett.125.015001

**Introduction.**—Understanding the scaling of plasma energy confinement time as a function of hydrogenic isotope mass is an important theoretical challenge for fusion research. Whereas most tokamak experiments operate with deuterium as the main ion species, fusion reactors will use a 50:50 deuterium-tritium fuel composition to increase the thermonuclear reaction cross section. The initial commissioning of ITER [1] calls for three phases of isotope operation: (1) dominant-hydrogen operation, (2) dominant-deuterium operation, and finally (3) deuterium-tritium operation. Thus, establishing a theoretical framework for transport scaling with plasma ion compositions ranging from hydrogen (H) to deuterium (D) to deuterium-tritium (DT) will be of significant value in planning the ramp-up stages to reactor-level operation.

Experiments in present-day tokamaks generally find an increase in the global energy confinement time with increasing hydrogenic isotope mass [2–4]. This favorable scaling contradicts simple theoretical arguments, and is a long-standing problem known as the *isotope effect*. Some theoretical mechanisms have recently been demonstrated to explain these disagreements (e.g., collisions [5],  $\mathbf{E} \times \mathbf{B}$  flow shear [6], electromagnetic fluctuations [6,7], and kinetic electrons [8–11]), but no general theoretical framework to explain these discrepancies has been proposed. In this Letter, we present such a theoretical framework for understanding the role of the nonadiabatic electron drive in the isotopic dependence of turbulent plasma transport, which is responsible for most thermal and particle loss in magnetically confined plasmas. In doing so, we quantify the dependence of energy transport on the electron-to-ion mass ratio  $m_e/m_i$  and its role in altering the ion-mass scaling of the turbulent flux from the core to the edge.

**Naive gyro-Bohm scaling.**—For clarity and to avoid nonessential physical mechanisms, we restrict our attention to a pure plasma  $n_e = n_i = n_0$  with equal temperature

$T_e = T_i = T_0$ . Dimensional analysis, based solely on the ion gyrokinetic equation [12] (and using the ion gyroradius as the characteristic length scale), predicts that the turbulent ion energy flux scales as

$$Q_i = c_0 Q_{\text{GB}i} \quad \text{where } Q_{\text{GB}i} = Q_{\text{GBD}} \sqrt{m_i/m_D}. \quad (1)$$

Here, the subscript  $i$  is the ion species index,  $Q_{\text{GBD}} \doteq n_0 T_0 v_D \rho_{*D}^2$  is the deuterium gyro-Bohm energy flux,  $v_D = \sqrt{T_0/m_D}$  is the deuterium thermal velocity,  $\rho_{*D} = (v_D/\Omega_{D,\text{unit}})/a$  is the deuterium ion-sound gyroradius normalized by the system size, and  $\Omega_{D,\text{unit}} = eB_{\text{unit}}/(m_D c)$  is the deuterium cyclotron frequency. In this limit,  $c_0$  is species independent (depending only on the density and temperature gradients, magnetic equilibrium geometry, etc.) and Eq. (1) predicts that the turbulent ion energy flux scales with the square root of the ion mass, such that  $Q_H < Q_D < Q_{\text{DT}}$ . This implies that the global energy confinement degrades with increasing ion mass, in contradiction with the general experimental trend.

This simple scaling—which we hereafter refer to as the *naive gyro-Bohm scaling*—is based on the physically unrealistic assumption of adiabatic electrons. When kinetic electron dynamics are properly retained in the gyrokinetic turbulence analysis, we expect the more complicated scaling,

$$Q_i = \tilde{c}_0(m_e/m_i) Q_{\text{GB}i}, \quad (2)$$

where the function  $\tilde{c}_0$  can have a strong dependence on mass ratio [8,11] in addition to all other dimensionless plasma parameters. In what follows, using nonlinear gyrokinetic turbulence simulations based on a DIII-D discharge, we illustrate a remarkable transition in the isotope mass scaling caused by the *nonadiabatic* response

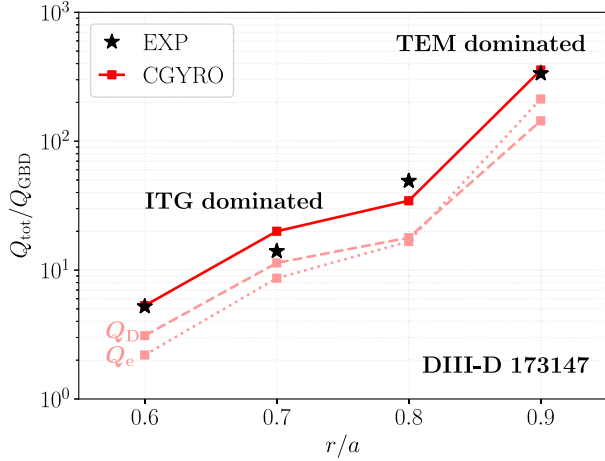


FIG. 1. Total energy flux ( $Q_e + Q_D$ ) comparing CGYRO turbulence simulations with experimental DIII-D power balance. The rapid increase at  $r/a = 0.9$  (note the log scale) is driven by nonadiabatic electron physics and is highly sensitive to the electron-to-ion mass ratio, and also to the safety factor  $q$ .

of electrons. This nonadiabatic response strongly regulates the turbulence levels and can in some cases (particularly in the plasma edge) dominate and favorably reverse the naive scaling so that  $Q_H > Q_D > Q_{DT}$ , in agreement with the experimental trend.

*Core-to-edge validation of energy flux.*—To establish an experimentally credible baseline scenario, we consider DIII-D discharge 173147 at  $t = 1705$  ms, a low-power Ohmically heated  $L$ -mode (low-confinement mode) deuterium plasma [13] at high density. Gyrokinetic simulations of the turbulent energy flux were carried out with the CGYRO code [14] over the range  $0.6 \leq r/a \leq 0.9$ . CGYRO solves the  $\delta f$  nonlinear gyrokinetic-Maxwell equations [12,15] using an Eulerian numerical scheme. In the simulations, the previously stipulated approximations are used, namely, a pure plasma with equal ion and electron temperatures. The experimental temperature gradient scale lengths are retained, while  $d \ln n_i / dr = d \ln n_e / dr$  based on quasineutrality. Shaped Miller geometry [16] is used, and collisions are included using the Sugama collision operator [17]. Electromagnetic fluctuations and rotation are retained, though these have only a minor influence. For the numerical resolution, the simulations use a box with perpendicular lengths  $L_x = L_y \sim 90\rho_i$  with  $N_r = 324$  radial modes and  $N_y = 16$  complex toroidal modes, resolving up to  $k_{\theta}\rho_i = 1$ .

Power-balance (target) energy fluxes are computed from the transport code TGYRO [18] using the experimental power and density sources. Despite the approximations, Fig. 1 shows that CGYRO matches the total (ion + electron) experimental power-balance flux over a broad radial range, in both the ion-dominated core ( $r/a \leq 0.8$ ), where  $Q_e \sim 0.7Q_i$ , and in the electron-dominated edge ( $r/a \sim 0.9$ ), where  $Q_e \sim 1.5Q_i$ . We have verified that

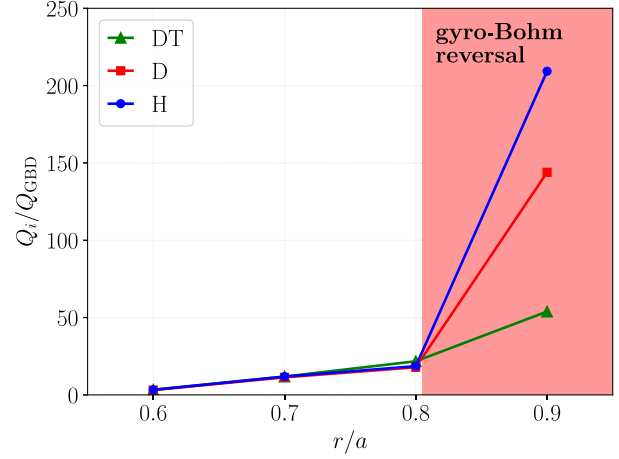


FIG. 2. Nonlinear ion energy flux comparing hydrogen, deuterium, and 50:50 DT plasmas. Note that the normalization has fixed deuterium gyro-Bohm units. A favorable reversal of the naive scaling, Eq. (1), is observed in the TEM-dominated edge.

the dominant linear instability in the core is an ion-temperature-gradient (ITG) mode, whereas in the edge it is an electron-temperature-gradient-driven trapped-electron mode (TEM).

*Violation of naive scaling.*—Figure 2 compares the simulated deuterium ion energy fluxes against hydrogen ( $m_H/m_D = 0.5$ ) and against 50:50 DT (treated as a single species with  $m_{DT}/m_D = 1.25$ ), with all other experimental equilibrium profile parameters fixed. In the ITG-dominated regime we observe  $Q_H \sim Q_D \sim Q_{DT}$ , suggesting that the naive gyro-Bohm scaling is broken (the fluxes have negligible mass dependence). In the TEM-dominated regime, a significant reversal from the naive scaling is found, with  $Q_H \gg Q_D \gg Q_{DT}$ . This implies that the hydrogen confinement relative to deuterium is significantly worse than expected by the naive mass scaling, whereas the DT scaling is better than expected. The electron energy fluxes (not shown) notably follow the ion-mass scaling of the ion fluxes. In what follows, we will examine these results more closely and propose an explicit form for the finite- $m_e/m_i$  corrections to Eq. (1).

*Finite electron-mass dynamics.*—The electron-mass dependence of the turbulent flux enters in five physically distinct ways: the electron parallel motion, electron-ion collisions, plasma rotation, electromagnetic fluctuations, and finite electron Larmor radius (FLR). For simplicity we neglect the latter two (electromagnetic and FLR) which we have verified do not play a critical role in the present discharge. To understand the origins of gyrokinetic isotope scaling in connection with the remaining terms—parallel motion, collisions, and rotation—we write the ion and electron gyrokinetic equations in dimensionless form:

$$\frac{\partial H_i}{\partial \tau_i} + \frac{u_{\parallel}}{qR} \frac{\partial H_i}{\partial \theta} = G_i(H_i, \Phi, \mathbf{p}), \quad (3)$$

$$\frac{\partial H_e}{\partial \tau_i} + \sqrt{\frac{m_i}{m_e}} \frac{u_{\parallel}}{q\mathcal{R}} \frac{\partial H_e}{\partial \theta} = G_e(H_e, \Phi, \mathbf{p}), \quad (4)$$

where  $\tau_i = (v_i/a)t$  is the time normalized to the ion-sound timescale,  $u_{\parallel} = v_{\parallel}/v_i$ , and  $\mathcal{R}$  is a dimensionless geometric factor that reduces to the normalized major radius  $R/a$  in a circle.  $H_i$  and  $H_e$  are the nonadiabatic ion and electron distributions [14] and  $\Phi = e\phi/T_0$  is the short-wavelength electrostatic potential. The terms  $G_i$  and  $G_e$  represent the totality of remaining terms in the equations—none of which have explicit electron-to-ion mass-ratio dependence. In writing these terms we ignore a very weak dependence of  $G_i$  on  $H_e$ , and  $G_e$  on  $H_i$ , from the collision operator. Importantly, we have introduced a vector  $\mathbf{p}$  of dimensionless parameters that are considered to be independent of the electron-to-ion mass ratio:

$$\mathbf{p} = \left[ \begin{array}{l} q, s, \epsilon, \kappa, \kappa', \dots, \quad (\text{geometry}) \\ \frac{T_e}{T_i}, \frac{a}{L_{Te}}, \frac{a}{L_{Ti}}, \dots, \quad (\text{profile}) \\ \frac{a\gamma_E}{v_i}, \frac{a\gamma_p}{v_i}, \dots, \quad (\text{rotation}) \\ \frac{a\nu_{ee}}{v_i}, \frac{a\nu_{ei}}{v_i}, \dots \end{array} \right] \quad (\text{collisions}), \quad (5)$$

where  $1/L_{Ta} \doteq -d\ln T_a/dr$  is the inverse temperature gradient scale length,  $\nu_{ee} \doteq \sqrt{2}\pi e^4 n_e \ln \Lambda / (m_e^{1/2} T_e^{3/2})$  is the electron collision rate,  $\gamma_E \doteq -(r/q)d\omega_0/dr$  is the  $\mathbf{E} \times \mathbf{B}$  shearing rate,  $\gamma_p = -Rd\omega_0/dr$ , and  $\omega_0$  is the toroidal rotation frequency. When writing the equations in this form, there is only a single irreducible term—the electron parallel motion—that can be responsible for ion-mass dependence of  $Q_i/Q_{GBi}$ . In other words, when held constant in ion units, the apparent dependence of collisions and rotation on mass ratio is removed.

In the limit  $m_e/m_i \rightarrow 0$  (sometimes called the zero-electron-mass limit [19]) the solution of Eq. (4) is the bounce-averaged distribution  $\langle H_e \rangle_b$  [20,21]. We remark that  $\langle H_e \rangle_b$  is associated with trapped electrons only, and is independent of  $m_e/m_i$  and therefore cannot modify the naive scaling. Corrections to this limit are formally obtained by expanding the nonadiabatic part of the electron distribution as an asymptotic series in the small parameter  $\omega/\omega_{be}$  [20,22], where  $\omega_{be}$  is the electron bounce frequency. Along these lines, we introduce the related but explicit ordering parameter

$$\epsilon \doteq q\mathcal{R} \sqrt{\frac{m_e}{m_i}}. \quad (6)$$

Although an asymptotic solution is completely intractable in the general case, we can nevertheless follow the

arguments of Ref. [23], and posit that the electron distribution admits the following series expansion:

$$H_e = \langle H_e \rangle_b + \epsilon H_e^{(1)} + \epsilon^2 H_e^{(2)} + \dots \quad (7)$$

In this expression, the correction terms  $H_e^{(n)}$  contain both trapped and passing electron contributions. This form of the solution suggests that the ion and electron energy fluxes have the form

$$\frac{Q_i}{Q_{GBi}} = c_0(\mathbf{p}) + c_1(\mathbf{p})\epsilon + c_2(\mathbf{p})\epsilon^2 + \dots, \quad (8)$$

$$\frac{Q_e}{Q_{GBi}} = d_0(\mathbf{p}) + d_1(\mathbf{p})\epsilon + d_2(\mathbf{p})\epsilon^2 + \dots, \quad (9)$$

where  $c_j(\mathbf{p})$  and  $d_j(\mathbf{p})$  are functions of all system parameters *except* the electron-to-ion mass ratio. When expressed in terms of fixed (deuterium) gyro-Bohm units, the series for  $Q_i$  yields

$$\frac{Q_i}{Q_{GBD}} = \underbrace{c_0 \sqrt{\frac{m_i}{m_D}}}_{\text{naive gyro-Bohm}} + \underbrace{c_1 q\mathcal{R} \sqrt{\frac{m_e}{m_D}}}_{\text{weak nonadiabatic}} + \underbrace{c_2 (q\mathcal{R})^2 \frac{m_e}{\sqrt{m_i m_D}}}_{\text{strong nonadiabatic}}, \quad (10)$$

with an analogous equation for  $Q_e$ . In our experience the mass dependence is always monotonically increasing, meaning that all  $c_j$  and  $d_j$  are positive. Thus, reversal from naive gyro-Bohm mass scaling can occur when finite- $m_e/m_i$  corrections from the strong nonadiabatic terms dominate.

*Numerical verification of scaling behavior.*—To explore the validity of the semiempirical scaling law in Eq. (10), we follow the strategy of Ref. [23] and introduce a fictitious scaling parameter  $\lambda$  that divides the parallel motion term in the electron equation:

$$\frac{\partial H_e}{\partial \tau_i} + \frac{1}{\lambda} \sqrt{\frac{m_i}{m_e}} \frac{u_{\parallel}}{q\mathcal{R}} \frac{\partial H_e}{\partial \theta} = G_e(H_e, \Phi, \mathbf{p}). \quad (11)$$

By adjusting  $\lambda$  we can control the size of the nonadiabatic correction; that is,  $\lambda \rightarrow 0$  corresponds to the (bounce-averaged) naive gyro-Bohm limit. In the discussion that follows, the reader can think of increasing  $\lambda$  as increasing  $\sqrt{m_e}$  in the parallel motion only. We can confirm the qualitative validity of the scaling law in Eq. (10) by looking more closely at the edge parameters at  $r/a = 0.9$ , as shown in Fig. 3. In the weakly collisional limit [ $\bar{\nu}_e \doteq (a/v_i)\nu_{ee} = 0.01$ ] the values of  $(c_0, c_1)$  and  $(d_0, d_1)$  are maximized. The vertical-axis intercepts for  $Q_e$  in Fig. 3(a) and  $Q_i$  in Fig. 3(b) indicate that  $c_0 \sim 90$  and  $d_0 \sim 150$ . These intercepts correspond to the naive gyro-Bohm limit obtained at zero electron mass ( $\lambda = 0$ ). The second term in Eq. (10), referred to as the weak

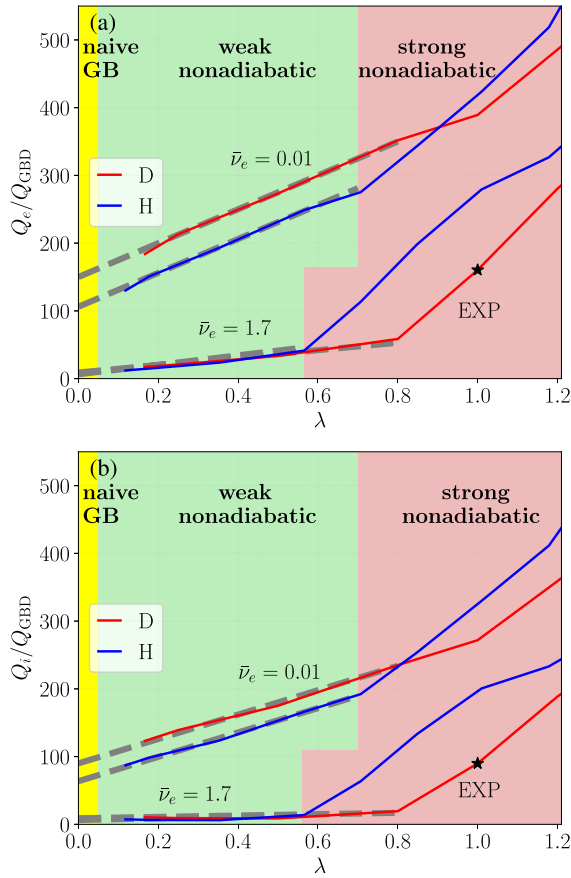


FIG. 3. Nonlinear (a) electron and (b) ion energy flux in the edge at  $r/a = 0.9$  comparing deuterium and hydrogen plasmas versus the (artificial) scaling parameter  $\lambda$  [see Eq. (11)] for the electron parallel motion. Naive gyro-Bohm scaling is recovered as  $\lambda \rightarrow 0$ . As  $\lambda$  increases, the turbulence transitions from a weakly nonadiabatic regime ( $Q_H < Q_D$ ) fit to Eq. (10) to first-order (gray dashed lines) to a strongly nonadiabatic regime ( $Q_H > Q_D$ ) where the finite- $m_e/m_i$  corrections drive a reversal of the naive gyro-Bohm scaling.

nonadiabatic effect, is independent of ion mass (when fluxes are expressed in mass-independent, fixed units). This term is illustrated by the parallel increase of the D and H curves in Fig. 3. In fixed  $Q_{GBD}$  units, the weak nonadiabatic term increases the flux by a constant amount that does not depend on ion mass. As such it cannot produce reversal from the naive gyro-Bohm scaling. Finally, as  $\lambda$  is increased further, the increase in flux becomes stronger than linear and the scaling enters the strong nonadiabatic regime, as expressed by the third term in Eq. (10), where reversed gyro-Bohm scaling ( $Q_H > Q_D$ ) is observed. We emphasize that the third term is only illustrative—we expect that the asymptotic series diverges in the strong nonadiabatic regime.

We remark that omitting  $\lambda$  from the  $k_y = 0$  (zonal) electron equation makes no significant difference to the simulated fluxes. In fact, it has been verified that the ratio of the nonzonal fluctuating potential to the zonal-flow

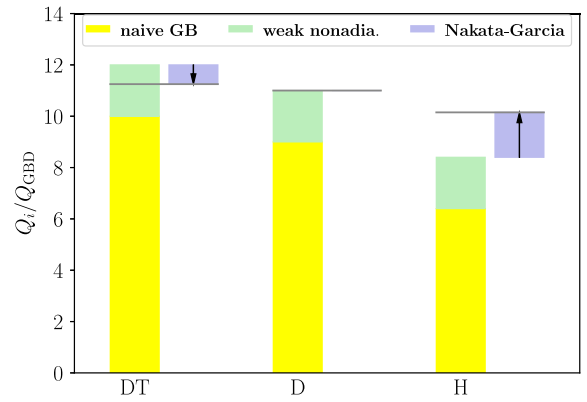


FIG. 4. Nonlinear ion energy flux in the ITG-dominated core at  $r/a = 0.7$  comparing hydrogen, deuterium, and 50:50 DT plasmas. Shown are the components of the flux due to the naive gyro-Bohm scaling (yellow) and the weak nonadiabatic contribution (green). Also shown (in blue) is the Nakata-Garcia effect that arises from keeping the collision and shearing rates fixed in absolute units. When these shearing rates are kept fixed in ion units, as in Eq. (5), the Nakata-Garcia effect vanishes.

potential is nearly independent of  $\lambda$  in Fig. 3 and ion species in Fig. 2. This feature of the fluctuations was analyzed in Ref. [23], demonstrating that zonal flows do not play a significant role in the mass-scaling behavior.

We observe that the trends just described in the weakly collisional case are preserved as  $\bar{\nu}_e$  is increased, but become more difficult to measure as the values for  $(c_0, c_1)$  and  $(d_0, d_1)$  drop. This drop is expected since collisions rapidly stabilize the TEM linear drive and thus the turbulent flux. Nevertheless, even when collision rates are increased by a factor of 170 ( $\bar{\nu}_e = 1.7$  in Fig. 3), and gyro-Bohm and weak nonadiabatic contributions are dramatically reduced, the relative flux enhancements seen in the strong nonadiabatic regime do not seem to be reduced. Furthermore, this analysis indicates that the experimental (D) operating point appears to be in the strong nonadiabatic regime, consistent with the original finding of Fig. 2. At fixed plasma gradients, the nonadiabatic effect is strongly enhanced at increased  $q$  and thus dominates in the plasma edge. Overall we claim that the high levels of energy flux observed in the  $L$ -mode edge are the result of strong nonadiabaticity of electrons that violates the naive gyro-Bohm scaling expectation. For this reason, it is unlikely that fluid or even bounce-averaged electron models will correctly describe edge isotope scaling.

The finite electron-mass correction is weaker in the core, where  $q$  is low and the driving gradients are small. This is shown in Fig. 4 for simulations at  $r/a = 0.7$ . At this radius, the nonadiabatic contribution (green shading) is dominated by the weak term and comprises only 25% of the total ion flux (for hydrogen). Despite some correction to the naive scaling, it is still observed that  $Q_H < Q_D < Q_{DT}$ . No reversal (as in the edge region in Fig. 2) is apparent. The dominant violation of the naive scaling at  $r/a = 0.7$ ,

which gives rise to  $Q_{DT} \sim Q_D \sim Q_H$  as observed in Fig. 2, is due to electron collisions, which more strongly stabilize heavier ions (at fixed  $\bar{v}_e$ ) [5]. A secondary stabilization mechanism is the  $\mathbf{E} \times \mathbf{B}$  flow shear, which more strongly quenches turbulence for heavier species (at fixed  $\gamma_E$ ) [6]. We refer to the sum of these two apparent isotope effects as the Nakata-Garcia effect. But, as observed earlier in Eq. (5), when collision and rotation shearing rates are rescaled with respect to the main ion timescale  $a/v_i$ , the Nakata-Garcia mass dependence (shown as the blue shaded bars in Fig. 4) is eliminated, leaving only the irreducible nonadiabatic correction to the ion flux.

*Summary.*—In this Letter we have proposed a new isotope-mass scaling law, Eq. (10), that describes the electron-to-ion mass ratio dependence of ion and electron energy fluxes in both ion-dominated core and electron-dominated edge transport regimes. The key findings are as follows. (1)  $m_e/m_i$  dependence arises from the nonadiabatic response associated with fast electron parallel motion. (2) Nonadiabatic electron drive strongly regulates the turbulence levels and plays a key role in altering—and in the case of the DIII-D  $L$ -mode edge, *reversing*—naïve gyro-Bohm scaling. (3) The finite electron-mass correction is larger for light ions and higher  $q$  so that, while it is weak in the core, it dominates the mass scaling in the edge.

For assessing the isotope scaling of global energy confinement in a reactor, it is essential to treat the electron parallel dynamics exactly. Fluid and/or bounce-averaged electron models [19,24] are unlikely to recover the correct ion-mass scaling. For a full transport analysis, additional influences (e.g., impurities, heating, magnetohydrodynamic activity) beyond the scope of this work must also be considered [25,26]. However, plasma confinement is known to be sensitive to edge conditions. Tokamak  $L$ -mode edge conditions typically lead to electron transport-dominated turbulence regimes such as studied here, for which the nonadiabatic electron drive is enhanced, resulting in a favorable reversal of the simple gyro-Bohm scaling with ion mass from H to D to DT. This has implications for lowering the power threshold for the  $L$ -mode (low-confinement mode) to  $H$ -mode (high-confinement mode) transition in a reactor like ITER, consistent with experimental observations comparing hydrogen and deuterium plasmas [27,28], and could trend the theoretical turbulent-based global energy confinement isotope scaling toward agreement with experimental observations.

This work was supported by the U.S. Department of Energy under Awards No. DE-FG02-95ER54309, No. DE-FC02-06ER54873 (Edge Simulation Laboratory), and No. DE-SC0017992 (AToM SciDAC-4 project). Computing resources were provided by the Oak Ridge Leadership Computing Facility under Contract No. DE-AC05-00OR22725 (ALCC program) and the National Energy Research Scientific Computing Center under Contract No. DE-AC02-05CH11231. This Letter was

prepared as an account of work sponsored by an agency of the U.S. Government. Neither the U.S. Government nor any agency thereof, nor any of their employees, makes any warranty, express or implied, or assumes any legal liability or responsibility for the accuracy, completeness, or usefulness of any information, apparatus, product, or process disclosed, or represents that its use would not infringe privately owned rights. The views and opinions of authors expressed herein do not necessarily state or reflect those of the U.S. Government or any agency thereof.

\*bellie@fusion.gat.com

- [1] B. Bigot, *Nucl. Fusion* **59**, 112001 (2019).
- [2] F. Tibone, B. Balet, M. Bures, J. Cordey, T. Jones, P. Lomas, K. Lawson, H. Morsi, P. Nielsen, D. Start, A. Tanga, A. Taroni, K. Thomsen, and D. Ward, *Nucl. Fusion* **33**, 1319 (1993).
- [3] M. Bessenrodt-Weberpals, F. Wagner, O. Gehre, L. Giannone, J. Hofmann, A. Kallenbach, K. McCormick, V. Mertens, H. Murmann, F. Ryter, B. Scorr, G. Siller, F. Söldner, A. Stähler, K.-H. Steuer, U. Stroth, N. Tsois, and H. Verbeek, and H. Zohm, *Nucl. Fusion* **33**, 1205 (1993).
- [4] ITER Physics Expert Group on Confinement and Transport, *Nucl. Fusion* **39**, 2175 (1999).
- [5] M. Nakata, M. Nunami, H. Sugama, and T.-H. Watanabe, *Phys. Rev. Lett.* **118**, 165002 (2017).
- [6] J. Garcia, T. Görler, F. Jenko, and G. Giruzzi, *Nucl. Fusion* **57**, 014007 (2017).
- [7] P. Manas, C. Angioni, A. Kappatou, F. Ryter, P. Schneider, and The ASDEX Upgrade Team, *Nucl. Fusion* **59**, 014002 (2019).
- [8] I. Pusztai, J. Candy, and P. Gohil, *Phys. Plasmas* **18**, 122501 (2011).
- [9] T. Hahm, L. Wang, W. Wang, E. Yoon, and F. Duthoit, *Nucl. Fusion* **53**, 072002 (2013).
- [10] A. Bustos, A. B. Navarro, T. Görler, F. Jenko, and C. Hidalgo, *Phys. Plasmas* **22**, 012305 (2015).
- [11] C. Angioni, E. Fable, P. Manas, P. Mantica, P. Schneider, ASDEX Upgrade Team, EUROfusion MST1 Team, and JET Contributors, *Phys. Plasmas* **25**, 082517 (2018).
- [12] E. Frieman and L. Chen, *Phys. Fluids* **25**, 502 (1982).
- [13] B. Grierson, C. Chrystal, S. Haskey, W. Wang, T. Rhodes, G. McKee, K. Barada, X. Yuan, M. Nave, A. Ashourvan, and C. Holland, *Phys. Plasmas* **26**, 042304 (2019).
- [14] J. Candy, E. Belli, and R. Bravenec, *J. Comput. Phys.* **324**, 73 (2016).
- [15] H. Sugama and W. Horton, *Phys. Plasmas* **5**, 2560 (1998).
- [16] R. Miller, M. Chu, J. Greene, Y. Lin-liu, and R. Waltz, *Phys. Plasmas* **5**, 973 (1998).
- [17] H. Sugama, T.-H. Watanabe, and M. Nunami, *Phys. Plasmas* **16**, 112503 (2009).
- [18] J. Candy, C. Holland, R. Waltz, M. Fahey, and E. Belli, *Phys. Plasmas* **16**, 060704 (2009).
- [19] F. Hinton, M. Rosenbluth, and R. Waltz, *Phys. Plasmas* **10**, 168 (2003).
- [20] F. Romanelli and S. Briguglio, *Phys. Fluids B* **2**, 754 (1990).
- [21] M. Beer and G. Hammett, *Phys. Plasmas* **3**, 4018 (1996).
- [22] F. Gang and P. Diamond, *Phys. Fluids B* **2**, 2976 (1990).

- [23] E. Belli, J. Candy, and R. Waltz, *Phys. Plasmas* **26**, 082305 (2019).
- [24] Y. Chen and S. Parker, *Phys. Plasmas* **8**, 441 (2001).
- [25] P. Schneider, A. Bustos, P. Hennequin, F. Ryter, M. Bernert, M. Cavedon, M. Dunne, R. Fischer, T. Görler, T. Happel, V. Igochine, B. Kurzan, A. Lebschy, R. McDermott, P. Morel, M. Willensdorfer, The ASDEX Upgrade Team, and The EUROfusion MST1 Team, *Nucl. Fusion* **57**, 066003 (2017).
- [26] J. Garcia, R. Dumont, J. Joly, J. Morales, L. Garzotti, T. Bache, Y. Baranov, F. Casson, C. Challis, K. Kirov, J. Mailloux, S. Saarelma, M. Nocente, A. Banon-Navarro, T. Görler, J. Citrin, A. Ho, D. Gallart, M. Mantsinen, and JET Contributors, *Nucl. Fusion* **59**, 086047 (2019).
- [27] F. Ryter, M. Cavedon, T. Happel, R. McDermott, E. Viezzer, G. Conway, R. Fischer, B. Kurzan, T. Pütterich, G. Tardini, M. Willensdorfer, and The ASDEX Upgrade Team, *Plasma Phys. Controlled Fusion* **58**, 014007 (2016).
- [28] C. Maggi *et al.*, *Plasma Phys. Controlled Fusion* **60**, 014045 (2018).